Technical Letter Report

Uncertainties in Seismic Hazard Assessment

Prepared by:

Mark Petersen
Oliver Boyd
Stephen Hartzell
Dan McNamara
Morgan Moschetti
Charles Mueller
Peter Powers
Sanaz Rezaeian
Allison Shumway

Other Contributors:

Jon Ake
Roland LaForge
Xiaodan Sun

NRC Contract Number NRC-HQ-60-11-I-0010

Rasool Anooshehpoor, NRC Project Manager

Office of Nuclear Regulatory Research

TABLE OF CONTENTS

LIST OF FIGURES

LIST OF TABLES

ABBREVIATIONS AND ACRONYMS

CENA	Central and Eastern North America
CEUS	Central and eastern United States
DBE	Design Basis Earthquake
EPRI	Electric Power Research Institute
GMI	Ground Motion Intensity
GMM	Ground Motion Model
GMPE	Ground Motion Prediction Equation
LLH	Log Likelihood
MLLH	Multivariate Log Likelihood
NGA	Next Generation Attenuation
NPP	Nuclear Power Plant
NRC	Nuclear Regulatory Commission
NSHM	National Seismic Hazard Model
PEER	Pacific Earthquake Engineering Research
PGA	Peak Ground Acceleration
PGV	Peak Ground Velocity
PSA	Pseudo-Spectral Acceleration
PSHA	Probabilistic Seismic Hazard analysis
RLME	Repeating Large-Magnitude Earthquake
SCR	Stable Continental Region
SSHAC	Senior Seismic Hazard Analysis Committee
USGS	United States Geological Survey

1 INTRODUCTION

United States Geological Survey (USGS) has been performing and evaluating probabilistic seismic hazard assessments (PSHA) that are used as independent validation of seismic hazard levels provided in nuclear power plant (NPP) applications and to evaluate the seismic conditions at existing reactor sites. Discrepancies between the results of NRC analyses and the analyses performed by industry have arisen and have resulted in a number of open items related to application reviews and points of disagreement between NRC staff and industry. This is a result, in part, of the significant uncertainties that exist in certain parameters and interpretations required to perform probabilistic seismic hazard assessments. These uncertainties are important in development of design basis earthquake (DBE) and in the assessment of seismic risk for existing facilities.

The purpose of this study is to further refine, understand and quantify the uncertainties that are intrinsic to PSHA studies in general, and the Central and Eastern United States (CEUS) in particular. The specific tasks in this study focus on:

- Development of a centralized database of recorded ground motion data in the Central and Eastern North America (CENA) and other appropriate stable continental regions (SCRs) that could be used in updating the ground motion models (GMMs) in CEUS.
- Simulation of ground motion time histories, over a wide range of magnitudes, using finite-fault models and using both deterministic physics-based method and site-based stochastic method to supplement scarce empirical data in CEUS.
- Comparative analysis of the USGS and NRC models for the CEUS PSHA to quantify the differences between the two and to better understand what components of each contribute to similarities and differences in calculated hazard.
- Implications of the increase in seismicity resulting from induced earthquakes in the CEUS on seismic hazard estimates and on the methodology used to incorporate induced seismicity and aftershocks into hazard estimates.
- Influence of foreshocks and aftershocks on hazard and the impact of current and new declustering algorithms on producing a statistically independent set of earthquakes in the CEUS, which could result in a better assessment of aftershock productivity and hazard, regional b-value, the rate of large mainshocks, and uncertainty in earthquake rates.

2 SUPPORT FOR NGA-EAST (TASK-1)

2.1 Background

The purpose of this task was to create a database containing earthquake data, station data, and ground motion data, in the NGA-East Project. This database is to be used in the development of new ground motion models for the CEUS. Task 1 was established to support two specific NGA-East activities (sub-activities). First sub-activity, was to develop an exhaustive database of recorded motions in CENA and other SCRs, with the associated metadata. The second sub-activity was to support general participation by USGS staff in the NGA-East SSHAC workshops and other activities to facilitate integration of NGA-East results with the National Seismic Hazard Mapping Program.

Activities:

1. Participate in development of a comprehensive database of recorded motions in CENA and other relevant SCRs.
2. Develop a flat file summarizing all relevant metadata (magnitude, distance, site conditions etc.).
3. Participate in NGA-East workshops and integration activities.

2.2 Deliverables

Charles Mueller led the research under this task. Working with Chris Cramer from the University of Memphis, Mueller led the initial development of the NGA-East database. He and Mark Petersen also participated in various NGA-East SSHAC workshops to guide the process. Information about the database and links to access the data and metadata can be found in the letter report.

Sub-activity 1 focused on the collection and curation of the CEUS data and metadata, beginning in late 2009 and essentially ending in mid-2011. C. Mueller of the USGS chaired this effort and did much of the work along with C. Cramer and others. USGS contributions were summarized in several presentations:

- Mueller gave two presentations at the NGA-East Database Working Group meeting, 11 Feb 2010, Berkeley, CA.
- Mueller gave three presentations at the NGA-East Database Working Group meeting, 09 Jun 2010, Berkeley, CA.
- Mueller, C., Cramer, C., and Toro, G., Status of the NGA-East ground motion database: NGA-East Project SSHAC meeting, 16 Nov 2010, Berkeley, CA.
- Mueller, C., Toro, G., Cramer, C., Kutliroff, J., and Dangkua, D. (2011). The NGA East ground motion database, SSA Annual Meeting, 13-15 April 2011, Memphis, TN (*SRL*, **82**, p. 287).

Sub-activity 2 focused more on waveform processing; USGS was not directly involved in sub-activity 2. This work was completed in 2014, and the data were made publically available at that time.

2.3 Final Report

The final report for this task is a PEER Report by Goulet et al. (2014):

Goulet, C.A., T. Kishida, T. D. Ancheta, C. H. Cramer, R. B. Darragh, W. J. Silva, Y. M. A. Hashash, J. Harmon, J. P. Stewart, K. E. Wooddell, and R. R. Youngs (2014). NGA-East Database, *PEER,* No. 2014/17.

The zip file containing the appendices to the report on the PEER website can be accessed by clicking the links NGA-East Database eAppendices (1-3) in '2014 Reports' folder of PEER Reports (PEER 2014/17 - PEER NGA-East Database). The appendices are:

a. Earthquake data: NGA-East_EarthquakeSourceTable_Public_20141118.xlsx
b. Ground motion data: NGA-East_RotD50_5pct_Flatfile_public_20141118.xlsx
c. Station data: NGA-East_StationDatabase_Public_20141118.xlsx

Abstract

This report serves as a documentation of the ground motion database development for the NGA-East Project. The ground motion database includes the two- and three-component ground-motion recordings from numerous selected events (M > 2.5, distances up to 1500 km) recorded in the CENA region since 1988. The final database contains over 29,000 records from 81 earthquake events and 1379 recording stations. The time series and metadata collected went through numerous rounds of quality assurance and review. The NGA-East database constitutes the largest database of processed recorded ground motions in SRCs.

The motivation behind the development of the empirical database is the same as for other NGA projects (NGA-West1 and NGA-West2), which is to be used, along with other information and data, for the development of ground motion prediction equations (GMPEs). The NGA-East ground motion database, similar to those from the NGA-West projects, includes pseudo-spectral acceleration (PSA) for the 5%-damped elastic oscillators with periods ranging from 0.01 to 10 sec. The preferred PSA measure used for the NGA-East GMPE development is RotD50, which is also provided for the same period range. Additionally, the NGA-East database includes Fourier amplitude spectra (FAS) of the processed ground motions. The NGA-East database therefore consists of three groups of complementary products: the summary file referred to as the flatfile, which contains metadata, ground motion information and intensity measures on a record-per-record basis, the time series (acceleration, velocity, and displacement), and the corresponding Fourier spectra files.

The primary objective of the database task was to provide the time series, response spectra, and Fourier spectra to the NGA-East GMPE developers. However, the NGA-East time series database will also be made available to the public through the PEER online ground motion tool. This report documents the data collection, processing, and development of data products for the NGA-East database.

3 ASSESSMENT OF IMPACT OF SINGLE-STATION AND PATH VARIABILITY MODELS (TASK-2)

3.1 Background

This task was designed to explore the potential benefits of using site-specific data and analytical models of the path-specific wave propagation and site-specific site response effects to estimate source-, path-, and site-specific ground motions. It was hoped that the results would help quantify the potential improvement in estimates of the total variability (σ_T).

3.2 Deliverables

USGS lost the employee it had tasked with doing this work shortly after the Interagency Agreement was finalized. As a result, little to no work was performed under this task, and the Interagency Agreement was modified, redirecting efforts to new Tasks 4.3, 5a, and 5b.

4 FINITE FAULT AND STOCHASTIC GROUND MOTION SIMULATIONS TO SUPPORT NGA-EAST (TASK-3)

4.1 Background

Estimation of median ground-motion and its variability is crucial in probabilistic seismic hazard analysis (PSHA). The probability of ground motion intensity (GMI) exceeding a certain level is dominated by the median predicted by the GMPE and the standard deviation of the GMPE that describes the variability of the data to the predicted median. However, the lack of an extensive dataset of empirical ground motion recordings for large-magnitude events at close distances in the CENA precludes a purely empirical approach to GMPE development. The objective of this task is to use a specific finite-fault simulation technique and a stochastic site-based technique to develop a broadband database of simulated ground motions to supplement the recorded data. Furthermore, due to the common assumption of a log-normal distribution in the GMPE regressions, the value of the GMI measure varies exponentially with an increase in the standard deviation. Consequently, even small variations in the standard deviation will have a pronounced impact on the results of a PSHA, especially at low probabilities of exceedance. Therefore, another objective of this task is to further understand, refine, and quantify the uncertainties that are intrinsic to PSHA studies in the CEUS.

4.2 Deliverables

4.2.1 Ground Motion Simulation

To supplement earthquake ground-motion recordings in the CEUS, USGS carried out two different approaches, (1) a deterministic physics-based method and a (2) site-based stochastic method, to simulate ground motions over a wide range of magnitudes. The research results were published in several journal articles (Sun *et al.*, 2015; Rezaeian *et al.*, 2017; Sun *et al.*, 2018a; Sun *et al.*, 2018b)

To validate the simulation techniques and to calibrate them for the CEUS region, Sun *et al.* (2015) used three broadband simulation methods to generate synthetic ground motions for the 2011 M_w5.8 Mineral, Virginia, earthquake, and compared them with the observed motions. The methods included a physics-based model by Hartzell et al. (1999, 2005), a stochastic source-based model by Boore (2009), and a stochastic site-based model by Rezaeian and Der Kiureghian (2010, 2012). The ground-motion dataset consisted of 40 stations within 600 km of the epicenter. Several metrics were used to validate the simulations: (1) overall bias of response spectra and Fourier spectra (from 0.1 to 10 Hz); (2) spatial distribution of residuals for GMRotI50 peak ground acceleration (PGA), peak ground velocity, and pseudo-spectral acceleration (PSA) at various periods; (3) comparison with ground-motion prediction equations (GMPEs) for the eastern United States.

The results (Figure 4-1) show that:

1. The physics-based model provides satisfactory overall bias from 0.1 to 10 Hz and produces more realistic synthetic waveforms.
2. The stochastic site-based model also yields more realistic synthetic waveforms and performs superiorly for frequencies greater than about 1 Hz.
3. The stochastic source-based model has larger bias at lower frequencies (<0.5 Hz) and cannot reproduce the varying frequency content in the time domain.

Rezaeian *et al.* (2017) used two of these simulation approaches, (1) the deterministic physics-based method and (2) the site-based stochastic method, to simulate ground motions over a wide range of magnitudes. Drawing on the results of Sun *et al*. (2015) as well as using the 2001 M_{w}7.6 Bhuj, India, earthquake, as a tectonic analog for a large magnitude CEUS event, they calibrated the two simulation methods over this magnitude range. Both models showed a good fit to the Mineral and Bhuj observations from 0.1 to 10 Hz (Figure 4-2 and Figure 4-3). Model parameters were then adjusted to obtain simulations for M_{w} 6.5, 7.0, and 7.6 events in the CEUS. The simulations were compared with the 2014 USGS weighted combination of existing ground-motion prediction equations in the CEUS. The physics-based simulations showed comparable response spectral amplitudes and a fairly similar attenuation with distance. The site-based stochastic simulations suggested a slightly faster attenuation of the response spectral amplitudes with distance for larger magnitude events and, as a result, slightly lower amplitudes at distances greater than 200 km. Both models were plausible alternatives and, given the few available data points in the CEUS, can be used to represent the epistemic uncertainty in modeling of postulated CEUS large-magnitude events.

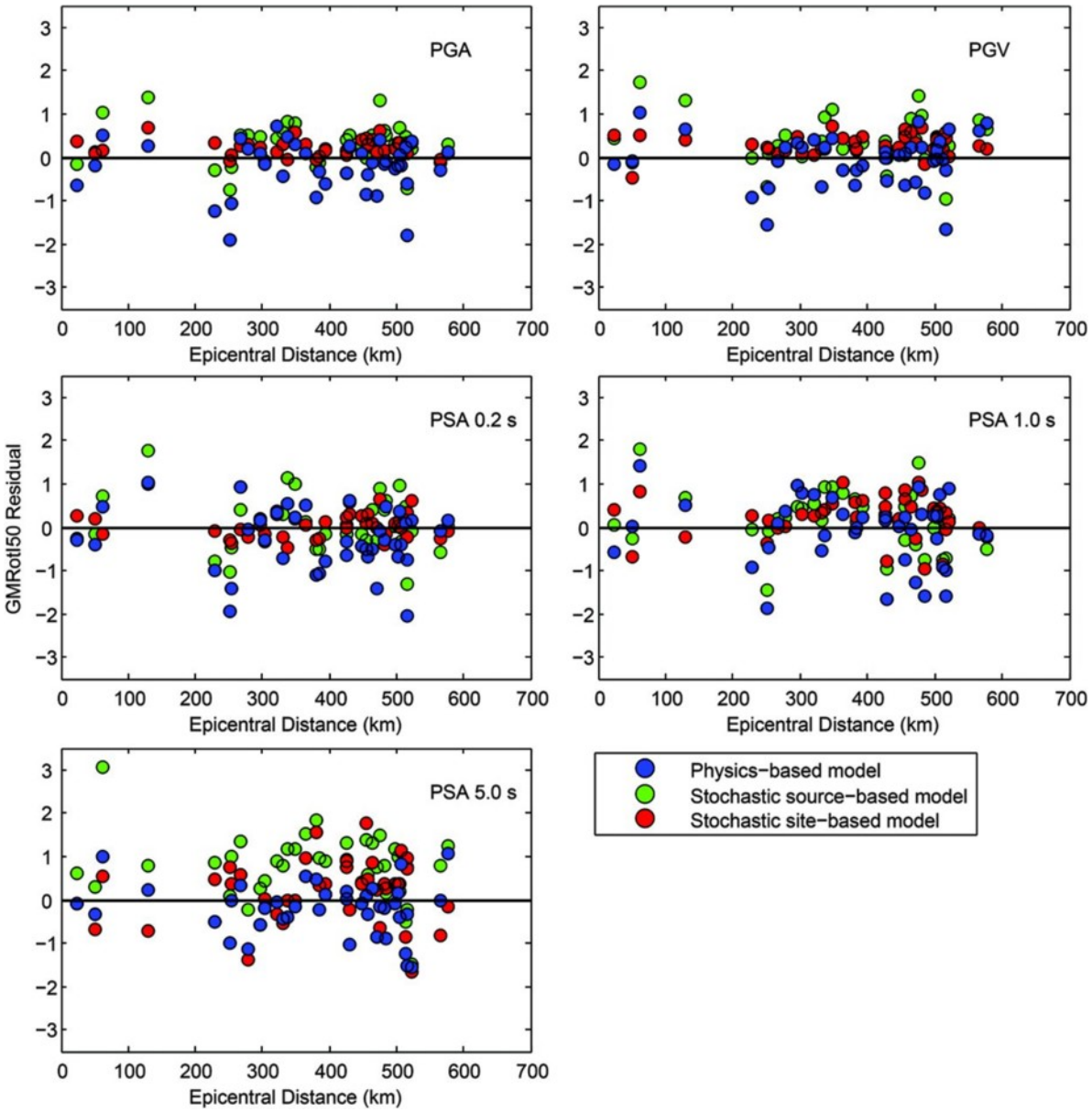

Figure 4-1: Natural log of GMRotI50 residuals for peak ground acceleration (PGA), peak ground velocity (PGV), and pseudospectral acceleration (PSA) at given periods versus distance for the three models (Sun *et al.*, 2015).

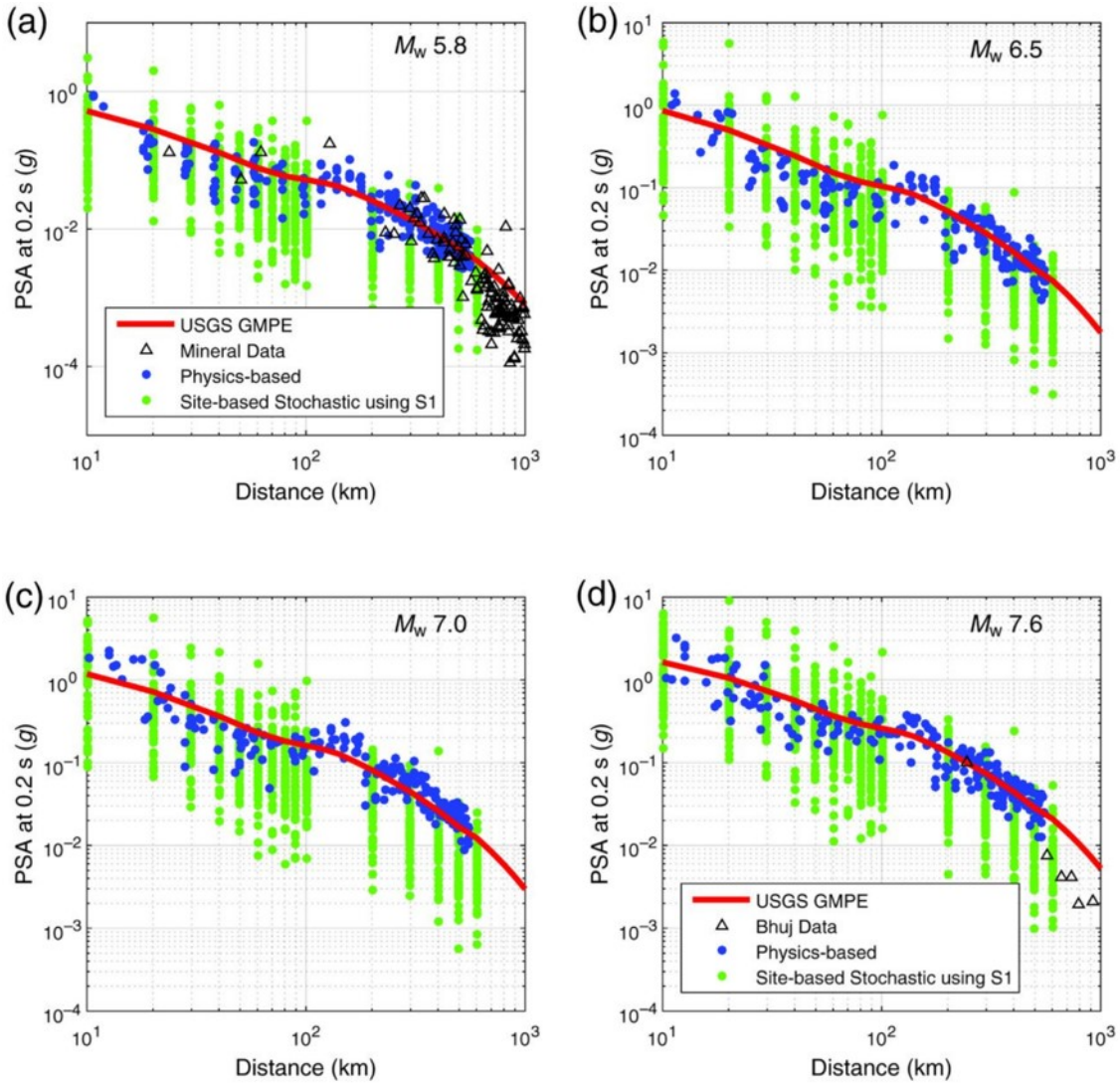

Figure 4-2: PSA at 0.2 s for the CEUS for M_w 5.8, 6.5, 7.0, and 7.6 events. The USGS 2014 GMPEs and data points from the Mineral and Bhuj earthquakes are superimposed for comparison.

.

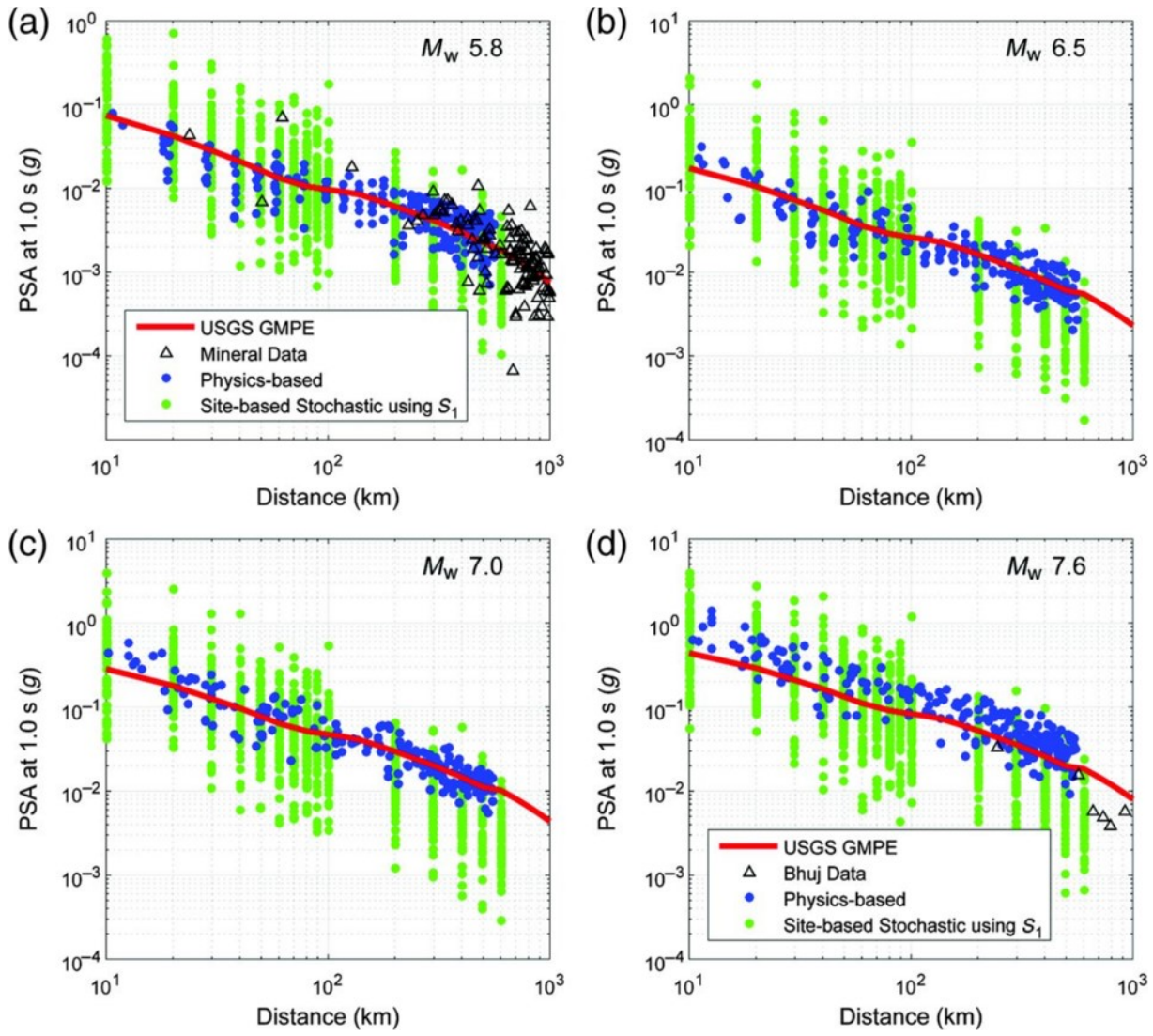

Figure 4-3: PSA at 1.0 s for the CEUS for M_w 5.8, 6.5, 7.0, and 7.6 events. The USGS 2014 GMPEs and data points from the Mineral and Bhuj earthquakes are superimposed for comparison

4.2.2 Ground Motion Uncertainties

The NGA-East project has adopted the Sammon's mapping approach for estimating epistemic ground motion uncertainties in the CEUS. Although this approach offers a convenient way of rendering a complex high-dimensional problem into a simpler lower-dimensional projection, the physics of the problem are obscured. Sun et al. (2018a and 2018b) used the two previous simulation approaches: (1) the deterministic physics-based method and (2) the stochastic site-based method to estimate the epistemic and aleatory ground-motion uncertainties in the CEUS and compared the results to those of the NGA-East (Sun et al., 2018a, 2018b).

For deterministic physics-based approach, using the NGA-East database, Sun et al. (2018b), simulated ground motions for the CEUS for magnitude earthquake scenarios M_w 6.0, 6.5, 7.0, 7.5, and 8.0. To estimate the uncertainty, they simulated realizations by varying rupture mechanism,

slip, stress drop, rupture velocity, source depth, and 1D velocity structure. The median spectral accelerations at various periods compared well with results from NGA-East. The synthetic median over all realizations is close to the 2014 National Seismic Hazard Model (NSHM) GMPEs for the CEUS in terms of amplitude and attenuation with distance. The synthetic median is relatively centered within the range of the 13 GMPEs from the NGA-East for USGS model. Standard deviation over all realizations ranges from 0.4 to 0.85 in natural log units (Figure 4-4). For most magnitudes, periods, and distances, the standard deviation falls in the range of those from the 2014 NSHM CEUS GMPEs. A larger within-event standard deviation, ϕ, than between-events standard deviation, τ, is observed for all magnitudes except for M_{w} 8.0. There is no clear trend of either total standard deviation with magnitude or ϕ with distance. The difference among standard deviations for different magnitudes becomes larger with increasing period, and so does the difference between τ and ϕ. A lower standard deviation and ϕ at closer fault distances and a larger τ than ϕ for some M_{w} 8.0 distances may indicate the need for a consideration of greater variation in model parameters such as slip distribution, station distribution and stress drop.

In the second method, Sun et al. (2018b) used the stochastic site-based simulation model. Six model parameters that represent the nonstationarity of ground motion in time- and frequency-domain were determined for available CEUS recordings. These estimated parameters were used to simulate ground motions for magnitude earthquake scenarios M_{w} 6.0, 6.5, and 7.0. Another set of parameters, based only on the data from the 2011 M_{w} 5.8 Mineral earthquake and magnitude scaling factors from the M_{w} 7.6 Bhuj earthquake, was applied to simulate ground motions for two large magnitude earthquake scenarios M_{w} 7.5 and 8.0. The synthetic spectral acceleration medians were compared with the 2014 NSHM GMPEs for the CEUS and the 13 GMPEs from the NGA-East USGS model. The standard deviation was compared with those of the 2014 NSHM CEUS GMPEs and with the ergodic standard deviation adopted by the NGA-East USGS model. At short periods ($T \leq 0.2$s), the synthetic median agrees with the referenced GMPEs well in terms of amplitude and attenuation with distance. As period increases, the synthetic median attenuates faster with distance. The synthetic standard deviation from scaling the Mineral data ranges from 0.48 to 1.04 in natural log units, which is in general higher than the NGA-East for USGS model, but in most cases comparable to the results of Al Atik (2015) from the NGA-East project (Figure 4-5). The synthetic standard deviation from using the CENA data ranges from 0.92 to 1.75 in natural log units, which is relatively high compared to other existing models but is determined empirically from observations. There is no dependence of the standard deviation on magnitude and distance.

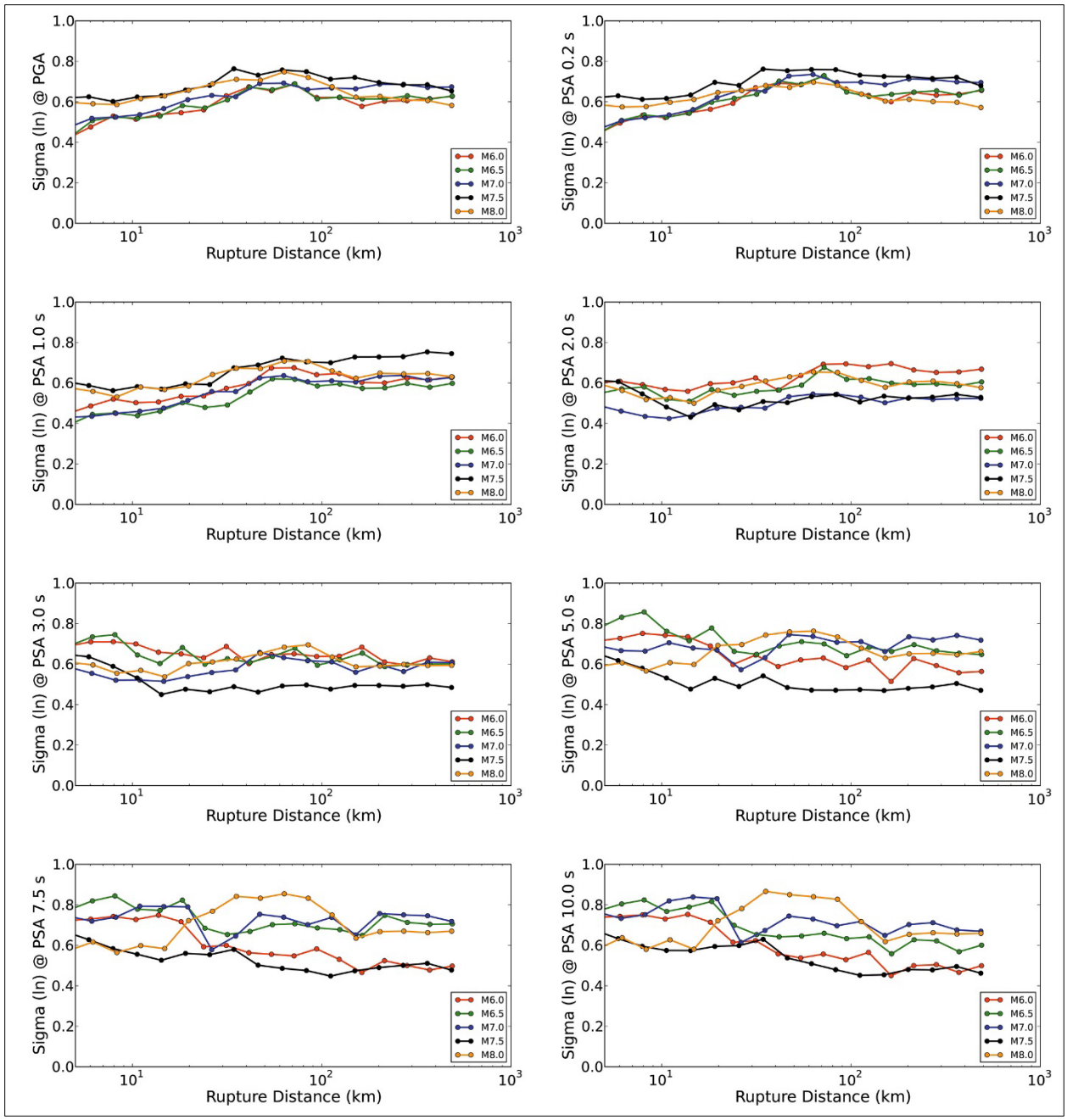

Figure 4-4: Sigma versus rupture distance at various periods and magnitudes.

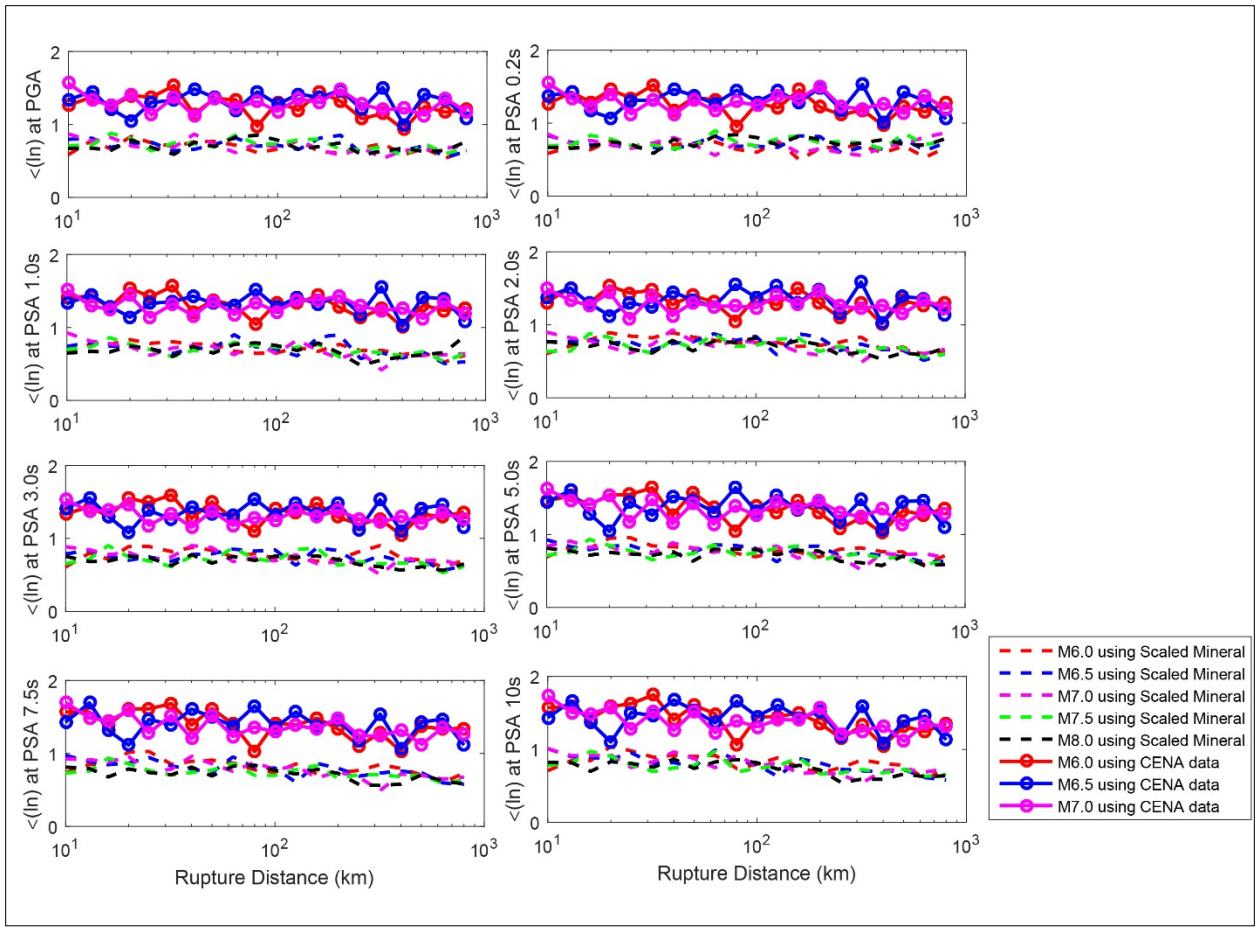

Figure 4-5: Sigma for all magnitudes using GMI measures. Solid curves represents the sigma from using CENA data whereas the dashed curves are those from scaling 2011 Mineral earthquake data.

4.3 References

Sun, X., S. Hartzell, and S. Rezaeian (2015). Ground-motion Simulation for the 23 August 2011, Mineral, Virginia, Earthquake Using Physics-Based and Stochastic Broadband Methods, *Bull. Seismo. Soc. Am.*, **105**, 2641-2661.

Rezaeian, S., S. Hartzell, X. Sun, and C. Mendoza (2017). Simulation of Earthquake Ground Motions in the Eastern United States Using Deterministic Physics-Based and Site-Based Stochastic Approaches. *Bull. Seism. Soc. Am.*, **107**, 149-168, doi:10.1785/0120160031.

Sun, X., B. Clayton, S. Hartzell, and S. Rezaeian (2018a). Estimation of ground motion variability in the Central and Easter United States: Part I. Using deterministic physics-based synthetics, *Bull. Seismo. Soc. Am.*, (submitted).

Sun, X., S. Rezaeian, B. Clayton, and S. Hartzell (2018b). Estimation of ground motion variability in the Central and Easter United States: Part II. Using stochastic site-based approach, *Bull. Seismo. Soc. Am.*, (submitted).

Al Atik L. (2015). NGA-East: Ground motion standard deviation models for Central and Eastern North America, *PEER* Report No. 2015/07, Pacific Earthquake Engineering Research Center, University of California, Berkeley, CA.

5 SENSITIVITY EVALUATION OF PSHA RESULTS (TASK-4)

5.1 Background

The USGS and NRC conducted a comparative analysis of their respective models for probabilistic seismic hazard analysis (PSHA) for the Central and Eastern United States (CEUS) to quantify the differences between the two and to better understand what components of each contribute to similarities and differences in calculated hazard. USGS calculations use the most recent update to the NSHM (Petersen et al., 2014), which prescribes both the source and ground-motion models (GMMs) to be used when computing hazard. The NRC calculations use their seismic-source characterization for the CEUS for nuclear facilities (Central and Eastern United States–Seismic Source Characterization, 2012) coupled with GMMs recommended by the Electric Power Research Institute (EPRI, 2013). In addition to comparing the total effect of source models and GMMs, both groups also computed hazard curves using a single GMM (Campbell, 2003), to determine if any observed differences could be solely attributed to variations between the two source models.

5.2 Comparison of USGS and NRC Seismic Hazard Models for the CEUS

5.2.1 Process and Parameters

The USGS and NRC calculated probabilistic seismic hazard at 73 sites throughout the CEUS that are largely coincident with major population centers. In selecting sites for analysis, consideration was given to sites that sample the hazard from

- Major fault-based sources, including sources of repeating large-magnitude earthquakes (RLMEs),
- Areas with elevated smoothed seismicity-source rates, or
- Areas with very low smoothed seismicity-source rates.

The sites selected and calculation parameterization are as follows:

Sites (73):

- For a list of sites, see https://github.com/usgs/nshmp-haz/blob/master/etc/nshm/sites-nrc.csv and https://github.com/usgs/nshmp-haz/blob/master/etc/nshm/sites-nrc.geojson.
- Site class: Hard Rock (V_{S30} = 2000 meters per second [m/s])

Intensity measures (spectral periods):

Peak ground acceleration (PGA) – NRC to use 100 Hz (0.01 s)

- Spectral acceleration (SA) of 10 Hz (0.1 s)
- SA of 5 Hz (0.2 s)
- SA of 1 Hz (1.0 s)

Ground-motion intensity levels (37):

[0.001, 0.00126, 0.00158, 0.002, 0.00251, 0.00316, 0.00398, 0.00501, 0.00631, 0.00794, 0.01, 0.0126, 0.0158, 0.02, 0.0251, 0.0316, 0.0398, 0.0501, 0.0631, 0.0794, 0.1, 0.126, 0.158, 0.2, 0.251, 0.316, 0.398, 0.501, 0.631, 0.794, 1.0, 1.26, 1.58, 2.0, 2.51, 3.16, 3.98] in units of gravity (g).

Maximum distance[*]:

- Grid (smoothed seismicity) sources: 500 kilometers (km)
- All others: 1000 km

Output format:

- Hazard values: Annual frequency of exceedance at the 37 ground-motion levels listed above.
- Curve files: Comma delimited (.csv)

5.2.2 Implementation Details and Differences

The following are implementation details of the USGS and NRC models that contribute to differences in hazard between the USGS and NRC results.

- Minimum magnitude (contributes to higher USGS rates at low end of hazard curves):
    - USGS, $M_W = 4.7$
    - NRC, $M_W = 5.0$
- Median ground-motion clamps (USGS only):
    - PGA or 100 Hz: 1.5 g
    - SA < 0.5 s: 3.0 g
- Maximum ground-motion clamps; the lesser of μ + 3σ and (USGS only):
    - PGA or 100 Hz: 3.0 g
    - SA < 0.75 s: 6.0 g
- Gridded seismicity-source discretization: USGS gridded seismicity sources are discretized at 0.1° in latitude and longitude. Many sites in this analysis are therefore coincident with a gridded seismicity source. Sites centered on 0.05° locations may therefore exhibit lower hazard (given the approximately 5 km distance from the nearest source) than one would get interpolating between adjacent 0.1°-centered sites that are co-located with sources. NRC discretizes at 0.25° with distance-dependent rediscretization.
- Gridded seismicity-source, rate-smoothing variants (for example, Gaussian fixed-kernel distance versus nearest-neighbor smoothing), seismicity floor or minimum rates (where applicable), and the minimum magnitudes and catalog durations (as a function of catalog completeness) used to compute grid-source Gutenberg-Richter a-values.
- Grid sources considered out to 320 km (200 miles) in NRC calculations versus 500 km in USGS calculations.
- Grid-source western extent:
    - USGS: 115°W
    - NRC: 105°W

[*] In the actual analysis, the distances considered for fault and grid sources in the NRC codes differed from those initially specified as detailed in the Implementation Details and Differences section.

- Maximum distance for faults: in the final analysis, NRC faults and RLMEs were considered at all sites, regardless of distance; USGS calculations only consider these sources out to 1000 km from a site.
- Ground-motion model logic-tree distance dependence: The USGS uses a logic tree of ground-motion models, the composition and weights of which change once the site-to-source distance is greater than 500 km. NRC uses the same logic tree at all site-to-source distances.
- The USGS codes use grid-source-optimization tables wherein earthquake rates are summed into fixed 5-km-distance bins such that the minimum site-to-source distance is 2.5 km. This means the minimum distance from a site to the surface projection of a rupture (r_{JB}) can never be less than 2.5 km and to the rupture plane (r_{Rup}) never less than 5.6 km, given fixed grid-source depths of 5 km.
- Differences in distance corrections for gridded seismicity-source model (or point-source) that are commonly used to approximate the distance to a fault of unknown strike. USGS codes do not apply any correction below $M_W = 6.0$.
- NRC uses spatially varying Gutenberg-Richter b-values.

5.2.3 Hazard-Curve Comparison

Work under this element is described in full in a separate Technical Letter Report to the U.S. Nuclear Regulatory Commission (Powers et al., 2017). What follows is a summary of this report.

This report is accompanied by four sets of hazard-curve data, two each computed with USGS and NRC codes. Both codes were used to compute curves at 73 sites considering their respective CEUS source and ground-motion models. A second set of curves was computed using both codes that only considered the Campbell (2003) GMM. Two sets of comparison plots were also generated, one each for the complete and Campbell-only models.

Annual rates of exceedance for USGS hazard curves are consistently higher (commonly by >20 percent) than those computed using NRC codes. Over most of the CEUS, gridded seismicity sources are the primary contributor to hazard. Whereas the USGS considers earthquakes down to $\boldsymbol{M}$4.7, the NRC minimum magnitude is $\boldsymbol{M}$5.0, which leads to significantly elevated earthquake rates for the USGS and consequently hazard, as illustrated by the curves from the Maryville, Tennessee, site (Figure 5-1). The Maryville site is located in the East-Tennessee seismic zone, where gridded seismicity earthquake rates are at their highest in the CEUS source model and USGS hazard is 70 to 100 percent higher than the NRC values (Table 5-1). This difference is entirely attributable to the gridded seismicity earthquake rates in the source model, as the equivalent plot comparing hazard using only the Campbell (2003) GMM shows a similar difference (Figure 5-2).

There are locations where hazard differences are as large as, or larger than, those observed at Maryville, for example at Cheyenne, Wyoming, and Denver, Colorado (Table 5-1). However, here the differences are due to the westernmost sources in the NRC model extending only to 105°W longitude whereas the USGS sources extend to 115°W; Denver and Cheyenne are located west of the limit of the NRC source model.

Over most of the CEUS, modeled earthquake rates are quite low, so although the USGS curves at varying return periods are commonly 20 to 60 percent higher than the NRC curves, the absolute difference in units of g are actually quite low; for example, see the Minneapolis, Minn.,

comparisons (Figure 5-3), which sample where the gridded seismicity-source-model earthquake rates are close to their floor, or minimum, values. At longer periods, the difference is further reduced (Figure 5-4), however the overall shapes of the USGS and NRC curves are different, likely reflecting an underlying difference in GMM behavior at longer periods, as confirmed by the Campbell-only comparison (Figure 5-5).

In areas influenced by higher-rate sources that are typically modeled as faults and that have commensurately higher hazard, there is good agreement (to within 20 percent) over the tails of curves (higher ground motions and lower rates) that reflect fault sources; for an example, see the Elgin, Oklahoma, comparisons (Figure 5-6). As with previous examples, the gridded seismicity-rate discrepancy is present at the upper end of the hazard curves (lower ground motions and higher rates). There is even better agreement over the curve tails at New Madrid, Missouri, especially at longer periods (Figure 5-7). At shorter periods the New-Madrid comparison plots reflect the clamps on maximum ground motion that the USGS imposes on CEUS GMMs at those periods (Figure 5-8).

5.2.4 Future Tasks

Following review of the curve comparisons and discussions between the USGS and NRC, the following possible next steps were agreed upon:

- Rate comparisons and de-aggregations (10 Hz, 5 Hz) at points:
  - Maryville, Tenn.
  - Charleston, S.C.
  - Cape Girardeau, Mo.
- Deterministic comparison of GMM(s) at different distances
- Rerun original comparisons with a minimum magnitude of $M_W = 5.0$
- Comparisons using fault and grid sources exclusive of one another
- Run Campbell (2003) comparisons using only single sources
- Decompose ground-motion differences into source and GMM components
- Examine differences in grid-source a-rate calculations
- Investigate why there is a difference in curve tails at New Madrid, Mo., in the Campbell comparison but not in the base-case comparison

5.3 References

Campbell, K.W. (2003). Prediction of strong ground motion using the hybrid empirical method and its use in the development of ground-motion (attenuation) relations in eastern North America, *Bull. Seismo. Soc. Am.*, **93**, 1012–1033.

Central and Eastern United States–Seismic Source Characterization (2012). Central and Eastern United States seismic source characterization for nuclear facilities: Palo Alto, California, U.S. Department of Energy, Electric Power Research Institute, and U.S. NRC [variously paged], accessed September 15, 2017 at http://www.ceus-ssc.com/Report/Downloads.html.

Electric Power Research Institute (2013). EPRI (2004, 2006) ground-motion model (GMM) review project: Electric Power Research Institute Technical Report, Product ID 3002000717, accessed September 15, 2017 at http://www.epri.com/abstracts/Pages/ProductAbstract.aspx?ProductId=000000003002000717.

Petersen, M.D., Moschetti, M.P., Powers, P.M., Mueller, C.S., Haller, K.M., Frankel, A.D., Zeng, Yuehua., Rezaeian, Sanaz, Harmsen, S.C., Boyd, O.S., Field, Ned, Chen, Rui, Rukstales, K.S., Luco, Nico, Wheeler, R.L., Williams, R.A., and Olsen, A.H. (2014). Documentation for the

2014 update of the United States National Seismic Hazard Maps: *USGS* Open-File Report 2014 –1091, 243 p.

Powers, P.M, Shumway, A., LaForge, R., Ake, J. (2017). Comparison of U.S. Geological Survey and Nuclear Regulatory Commission seismic hazard models for the Central and Eastern United States: Technical Letter Report to the U.S. Nuclear Regulatory Commission, 13pp.

Table 5-1: Summary of differences in hazard expressed as percentages (USGS relative to NRC). Values are shown for the four periods considered and at four return periods: 0.5, 2, 5, and 10 percent probability of exceedance in 50 years.

Site	Coordinates		PGA				0.01 s (10 Hz)				0.2 s (5 Hz)				1.0 s (1 Hz)			
	Latitude	Longitude	0.5%	2%	5%	10%	0.5%	2%	5%	10%	0.5%	2%	5%	10%	0.5%	2%	5%	10%
Atmore_AL	31.00	-87.50	13	9.7	16	26	11	3.7	4.6	11	19	17	21	29	33	35	39	44
Birmingham_AL	33.50	-86.80	60	50	40	38	51	43	35	34	54	43	37	40	37	35	37	42
El_Dorado_AR	33.20	-92.70	7.4	-0.79	4.5	13	4.2	-4.9	-2.7	5	12	10	15	21	30	31	32	34
Greenbrier_AR	35.20	-92.40	57	51	48	52	46	41	40	46	45	41	43	50	38	38	39	43
Little_Rock_AR	34.75	-92.30	26	19	21	29	19	16	19	26	22	23	28	35	34	34	35	37
Denver_CO	39.75	-105.00	69	86	110	130	63	81	110	130	68	84	110	130	65	73	80	91
La_Junta_CO	38.00	-103.55	11	-10	26	53	6.5	-6.3	27	52	12	7.5	41	63	15	18	27	34
Trinidad_CO	37.20	-104.50	31	30	46	75	24	27	45	74	32	35	54	79	30	34	38	44
Hartford_CT	41.75	-72.70	38	37	44	53	33	37	44	53	42	47	53	60	49	48	47	48
Washington_DC	38.90	-77.05	5.7	5.2	14	23	5.8	7.9	15	24	19	21	27	34	26	21	17	15
Wilmington_DE	39.75	-75.55	28	30	41	53	23	30	40	52	33	40	48	58	38	32	28	29
Jacksonville_FL	30.35	-81.65	5.8	10	20	30	5.3	5.2	12	22	17	19	26	35	32	31	32	35
Miami_FL	25.75	-80.20	100	81	70	69	99	84	68	63	92	74	67	68	19	11	2.3	-24
Atlanta_GA	33.75	-84.40	7.9	11	17	24	7.6	12	17	23	22	25	29	35	38	39	43	47
Lincolnton_GA	33.80	-82.50	92	89	66	44	81	77	55	39	84	73	57	47	52	45	45	48
Savannah_GA	32.10	-81.10	-3.9	-4.3	3.3	14	-2.9	-1.2	5.2	16	7.5	9.6	16	27	24	27	29	34
Des_Moines_IA	41.60	-93.60	-20	-11	2	11	-25	-28	-22	-14	-8.3	-2.3	5.1	12	27	31	34	35
Central_IL	40.00	-90.00	-49	-37	-27	-18	-43	-36	-29	-22	-22	-13	-5.2	-0.13	23	25	25	24
Chicago_IL	41.85	-87.65	-6.8	-13	-9.5	-0.25	-7	-14	-15	-13	3.6	0.46	3.7	8.8	29	31	33	31
Evansville_IN	38.00	-87.60	-0.83	-9.2	-14	-13	-7.7	-12	-14	-12	1.8	-0.49	1.1	3.5	21	24	24	21
Indianapolis_IN	39.80	-86.15	-14	-22	-21	-14	-14	-19	-20	-17	-1.9	-4.6	-1.9	2.4	22	25	26	25
Topeka_KS	39.05	-95.70	3.5	-10	-7.7	1.7	1	-14	-22	-18	8.9	-0.64	1.7	6.9	29	30	33	34
Wichita_KS	37.70	-97.35	-33	-19	-3.9	9.2	-29	-19	-11	-3.1	-11	-1.4	7.1	15	24	28	32	35
Louisville_KY	38.25	-85.75	-30	-32	-26	-18	-28	-30	-26	-21	-12	-8.7	-3.6	1.4	24	27	28	28
New_Orleans_LA	29.95	-90.05	7.3	6.3	14	23	7.4	2.4	2.2	6.7	15	13	17	24	29	31	34	35
Boston_MA	42.35	-71.05	44	45	52	62	37	42	51	61	47	51	58	65	51	51	52	53
Baltimore_MD	39.30	-76.60	2	6.7	19	31	1.9	10	20	30	14	22	31	40	26	21	18	17
Augusta_ME	44.30	-69.80	51	54	53	54	44	50	51	52	53	55	54	55	48	46	47	48
Bangor_ME	44.80	-68.80	61	58	51	48	53	53	48	46	60	57	51	49	48	45	45	46
Portland_ME	43.65	-70.25	39	40	44	50	32	38	43	49	42	47	50	54	46	46	47	48
Detroit_MI	42.35	-83.05	18	17	21	28	19	18	20	23	30	28	30	33	26	27	30	32
Minneapolis_MN	45.00	-93.30	30	35	42	52	30	30	33	36	38	39	41	47	17	22	29	34
Cape_Girardeau_MO	37.30	-89.50	-7.9	-10	-13	-19	-9.2	-10	-11	-17	1.8	1.5	-0.07	-6.5	18	21	19	8.5
New_Madrid_MO	36.60	-89.55	NA	-25	-20	-4.5	NA	NA	-23	-8.1	NA	-18	-15	-0.86	-0.48	0.18	1.9	7.6
St_Louis_MO	38.60	-90.20	20	5.1	-1.8	-1.3	11	0.53	-3.1	-1.5	15	9.9	11	13	26	28	27	26
Jackson_MS	32.30	-90.20	-11	-11	-2.3	6.6	-12	-16	-11	-2.4	0.59	3.3	9.3	17	27	29	31	32
Charlotte_NC	35.25	-80.85	-0.61	-3.6	2.3	10	-0.34	-1.7	2.8	9	12	14	18	24	32	33	35	40
Fargo_ND	46.90	-96.80	24	38	52	58	26	39	52	61	36	48	57	64	4.9	-18	-33	-38

Site	Coordinates		PGA				0.01 s (10 Hz)				0.2 s (5 Hz)				1.0 s (1 Hz)			
	Latitude	Longitude	0.5%	2%	5%	10%	0.5%	2%	5%	10%	0.5%	2%	5%	10%	0.5%	2%	5%	10%
Omaha_NE	41.25	-96.00	-16	-3.5	8.4	21	-11	-5.7	-0.66	5	2.4	8.7	14	21	22	26	31	36
Manchester_NH	43.00	-71.45	86	89	90	89	77	82	84	83	83	86	85	82	73	65	62	61
Trenton_NJ	40.20	-74.75	43	45	53	65	38	43	52	64	47	51	59	68	49	42	38	38
Artesia_NM	32.85	-104.40	-36	1.2	30	50	-29	4.4	29	47	-10	19	38	54	8.1	1	-7.6	-15
Batavia_NY	43.00	-78.20	66	66	61	56	59	62	59	53	66	65	60	55	46	35	29	27
Malone_NY	44.85	-74.30	24	26	26	29	15	20	23	27	24	28	31	36	23	29	33	37
New_York_NY	40.75	-74.00	27	44	62	79	21	40	59	76	33	49	64	76	45	45	43	42
Columbus_OH	39.95	-83.00	-45	-34	-20	-6.6	-40	-29	-19	-11	-22	-10	-1.2	6.9	21	26	30	33
Sidney_OH	40.30	-84.15	85	81	59	28	74	71	50	23	79	72	50	32	50	42	41	42
Youngstown_OH	41.10	-80.65	4.1	4.1	11	19	5.2	7.2	11	15	17	19	23	27	23	24	29	33
Elgin_OK	34.80	-98.30	19	-9.7	18	54	8.6	-14	19	52	15	-12	28	56	29	-3.5	21	39
Oklahoma_City_OK	35.50	-97.50	51	46	47	56	43	39	44	54	46	43	48	56	32	32	36	44
Philadelphia_PA	39.95	-75.15	32	33	44	57	27	33	44	57	37	43	52	62	42	36	32	33
Pittsburg_PA	40.45	-80.00	-13	-9.4	1.4	11	-8.5	-5.9	-0.36	5	7.1	11	17	22	22	24	29	34
Providence_RI	41.80	-71.40	46	45	50	58	41	43	49	58	50	52	57	64	52	51	50	51
Charleston_SC	32.80	-79.95	14	30	46	75	8.4	24	40	69	14	28	44	73	28	40	49	64
Edgemont_SD	43.30	-103.85	55	57	69	90	50	54	67	89	59	63	77	96	66	67	70	75
Platte_SD	43.40	-98.85	55	53	56	63	49	50	54	61	57	56	59	64	40	21	9.6	4.9
Sioux_Falls_SD	43.55	-96.75	9	18	32	46	10	20	32	43	24	33	41	50	22	24	30	38
Chattanooga_TN	35.05	-85.25	66	74	72	68	56	64	64	64	65	67	64	63	51	45	46	50
Knoxville_TN	35.95	-83.90	30	49	65	76	25	43	58	69	40	54	64	70	53	48	48	51
Maryville_TN	35.75	-84.00	71	91	100	110	62	80	91	95	73	87	93	93	74	64	60	60
Memphis_TN	35.15	-90.05	2.3	0.23	0.69	4.6	-2	-2.2	0.24	4.6	5.2	5.7	8.7	13	16	20	21	21
Amarillo_TX	35.20	-101.85	67	58	55	60	59	53	53	58	64	56	54	59	38	25	15	9.6
Dallas_TX	32.80	-96.80	0.11	6.4	17	31	0.86	3.8	11	22	12	16	24	34	27	29	34	40
Houston_TX	29.75	-95.35	64	52	52	59	58	48	44	44	59	48	47	51	28	29	34	41
Kermit_TX	31.85	-103.10	73	85	93	97	65	79	90	98	72	81	85	88	48	28	12	-1.3
San_Antonio_TX	29.40	-98.50	0.23	21	36	46	3.3	21	34	43	17	29	39	47	1.7	-5.6	-13	-25
Snyder_TX	32.70	-100.90	-36	-11	8.3	26	-29	-11	4.8	21	-11	5.4	19	34	8.4	5	3.9	5.3
Blacksburg_VA	37.25	-80.40	22	24	24	26	17	22	24	25	28	31	32	33	32	32	35	40
Richmond_VA	37.55	-77.45	30	30	32	36	23	27	30	34	33	36	37	39	33	27	23	19
Burlington_VT	44.50	-73.20	25	25	25	28	19	22	24	28	28	31	33	36	29	34	37	40
Milwaukee_WI	43.05	-87.90	-25	-13	-0.65	12	-20	-16	-11	-4.3	-4.8	0.63	7.6	15	24	27	31	31
Charleston_WV	38.35	-81.65	28	19	18	22	26	20	18	20	35	30	30	31	36	35	39	43
Cheyenne_WY	41.15	-104.80	63	85	100	120	61	82	100	120	70	88	110	120	74	78	84	93

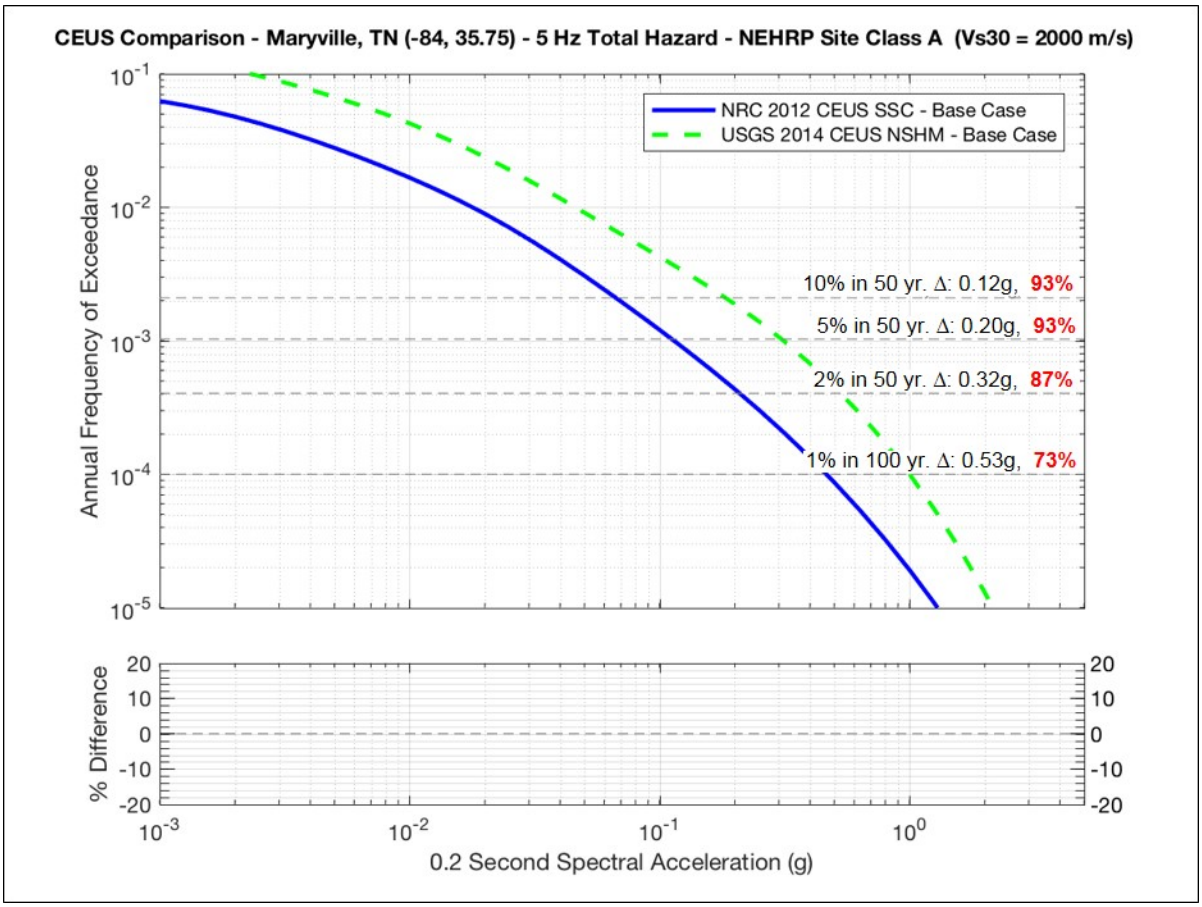

Figure 5-1: Comparison of USGS and NRC 5 Hz hazard curves, considering all ground-motion models, at Maryville, TN. The Maryville site is located in the East-Tennessee seismic zone where modeled earthquake rates are among the highest in the Central and Eastern United States. The numbers in red are the ratio of USGS to NRC ground-motion levels at the specified return periods. The lower plot shows the ratio of USGS to NRC exceedance rates over the entire curve; in this case, the ratios are out of range of the plot limits.

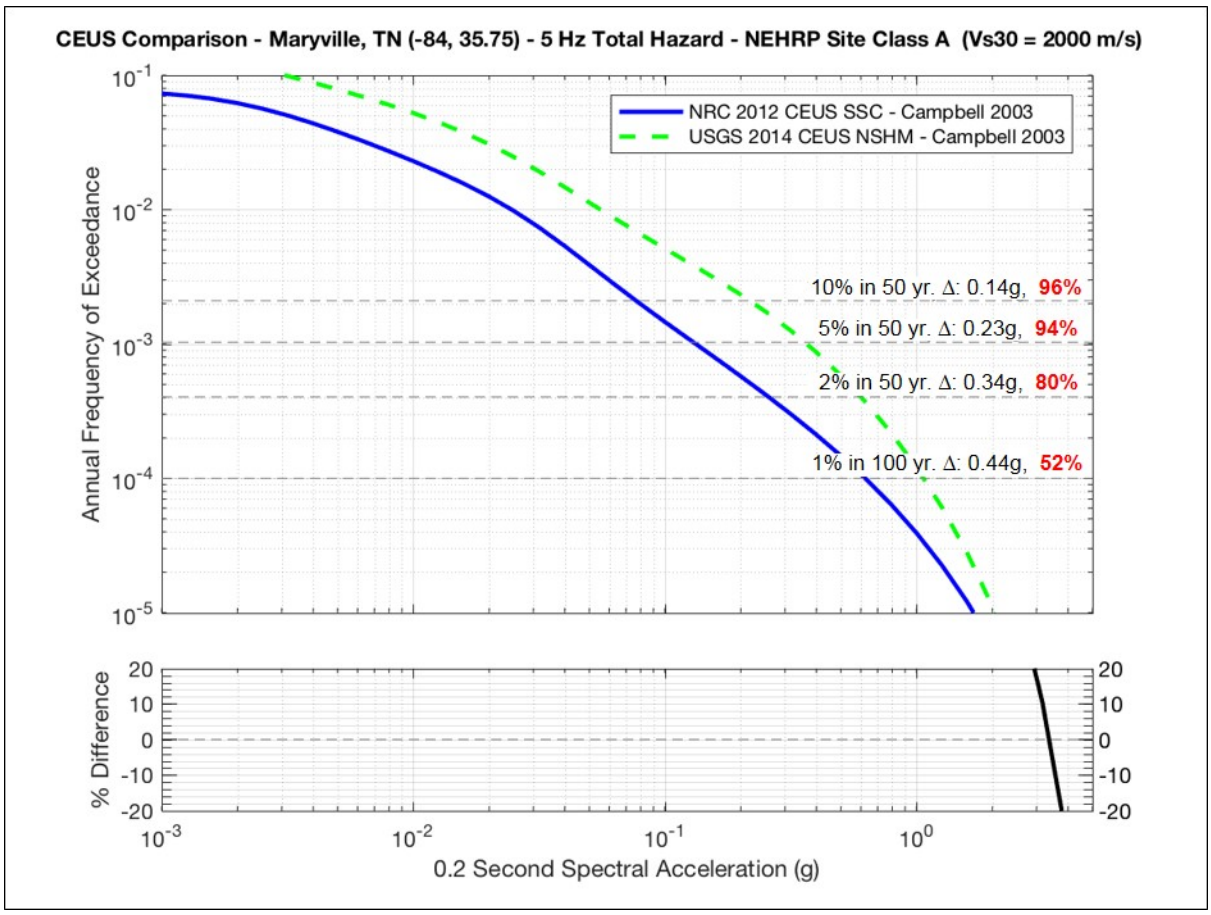

Figure 5-2: Comparison USGS and NRC 5 Hz hazard curves, considering only the Campbell (2003) ground-motion model, at Maryville, TN. The numbers in red are the ratio of USGS to NRC ground-motion levels at the specified return periods. The lower plot shows the ratio of USGS to NRC exceedance rates over the entire curve (the ratios are out of range of the plot limits).

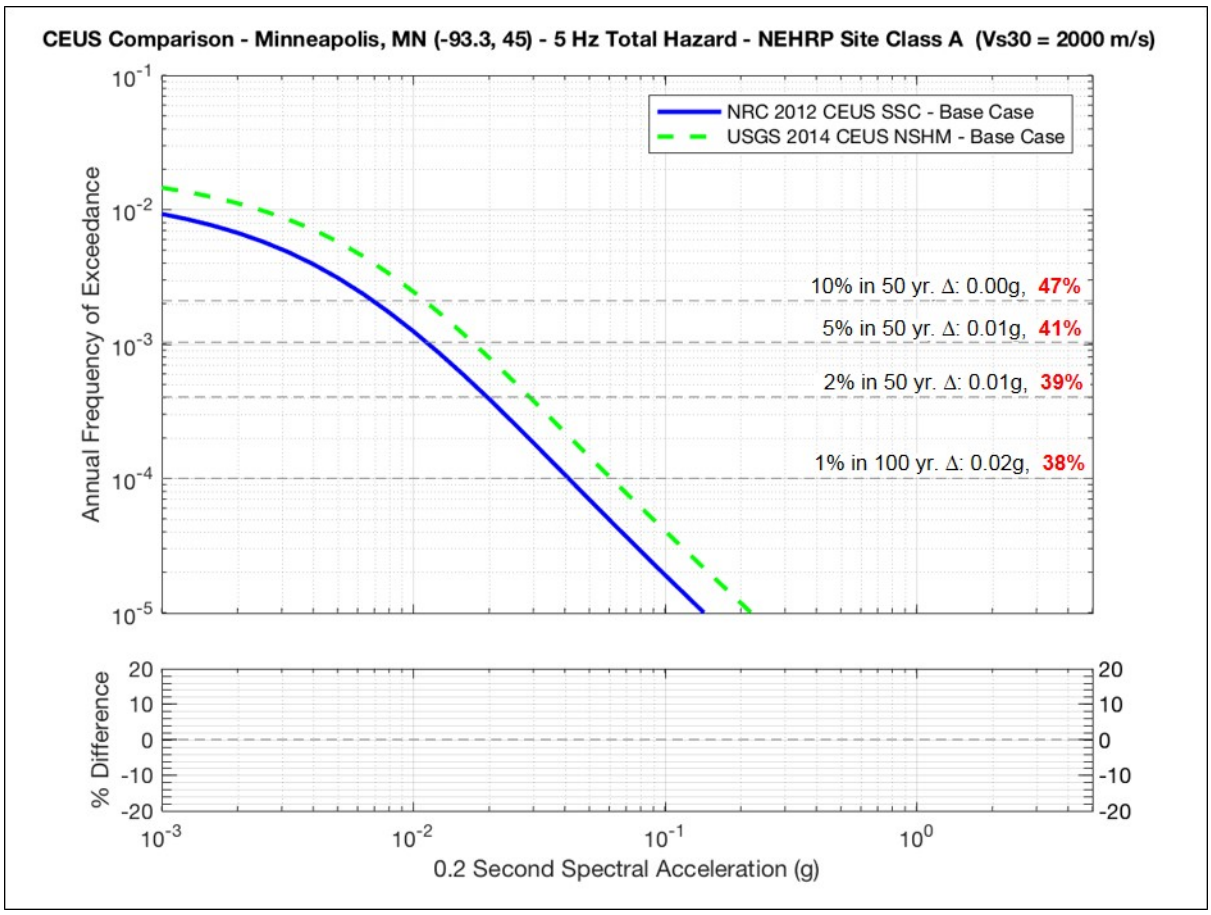

Figure 5-3: Comparison of USGS and NRC 5 Hz hazard curves, considering all ground-motion models, at Minneapolis, MN. The Minneapolis site is located where the USGS and NRC gridded seismicity source model earthquake rates are close to their floor, or minimum, rate. The numbers in red are the ratio of USGS to NRC ground-motion levels at the specified return periods. The lower plot shows the ratio of USGS to NRC exceedance rates over the entire curve (the ratios are out of range of the plot limits).

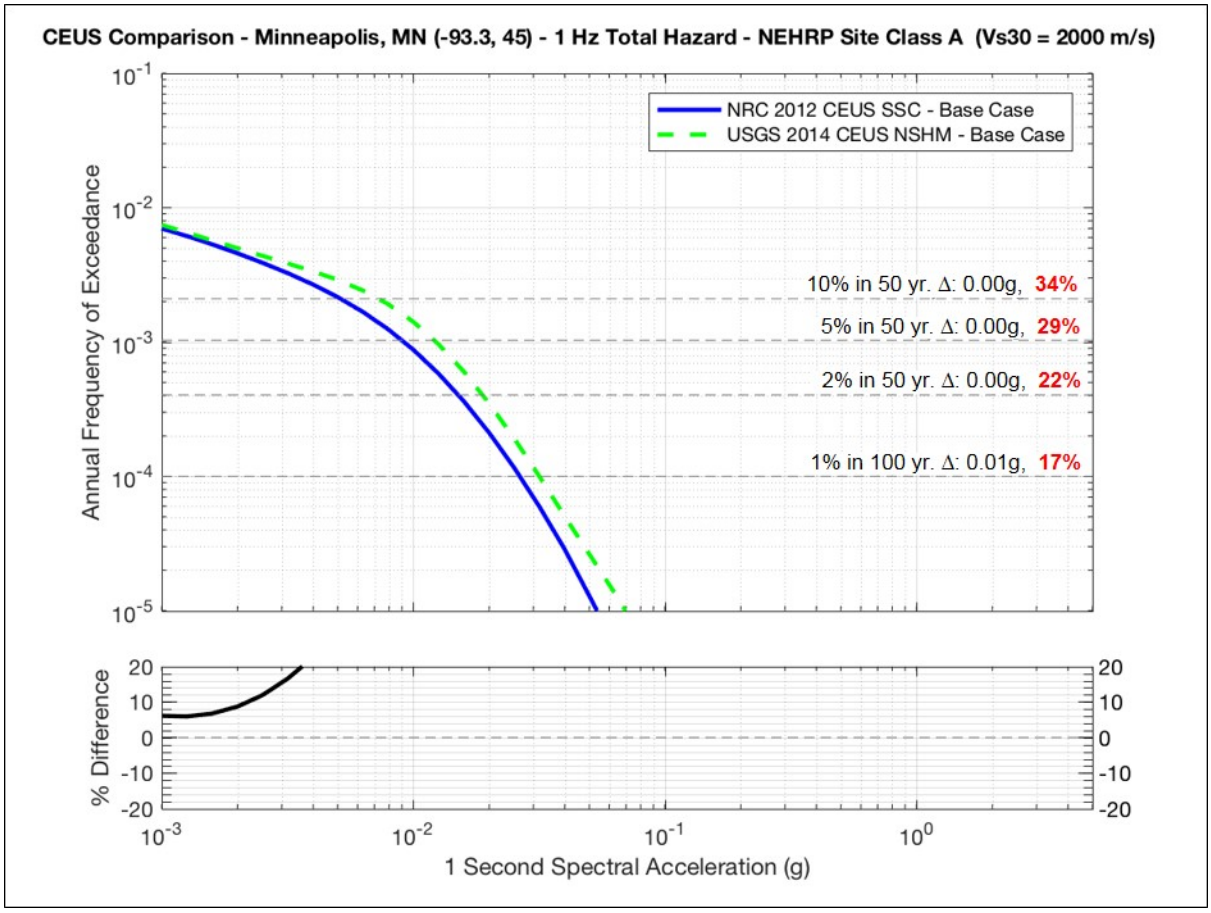

Figure 5-4: Comparison of USGS and NRC 1 Hz hazard curves, considering all ground-motion models, at Minneapolis, MN. The Minneapolis site is located where the USGS and NRC gridded seismicity source model earthquake rates are close to their floor, or minimum, rate. The numbers in red are the ratio of USGS to NRC ground-motion levels at the specified return periods. The lower plot shows the ratio of USGS to NRC exceedance rates over the entire curve (the ratios are out of range of the plot limits).

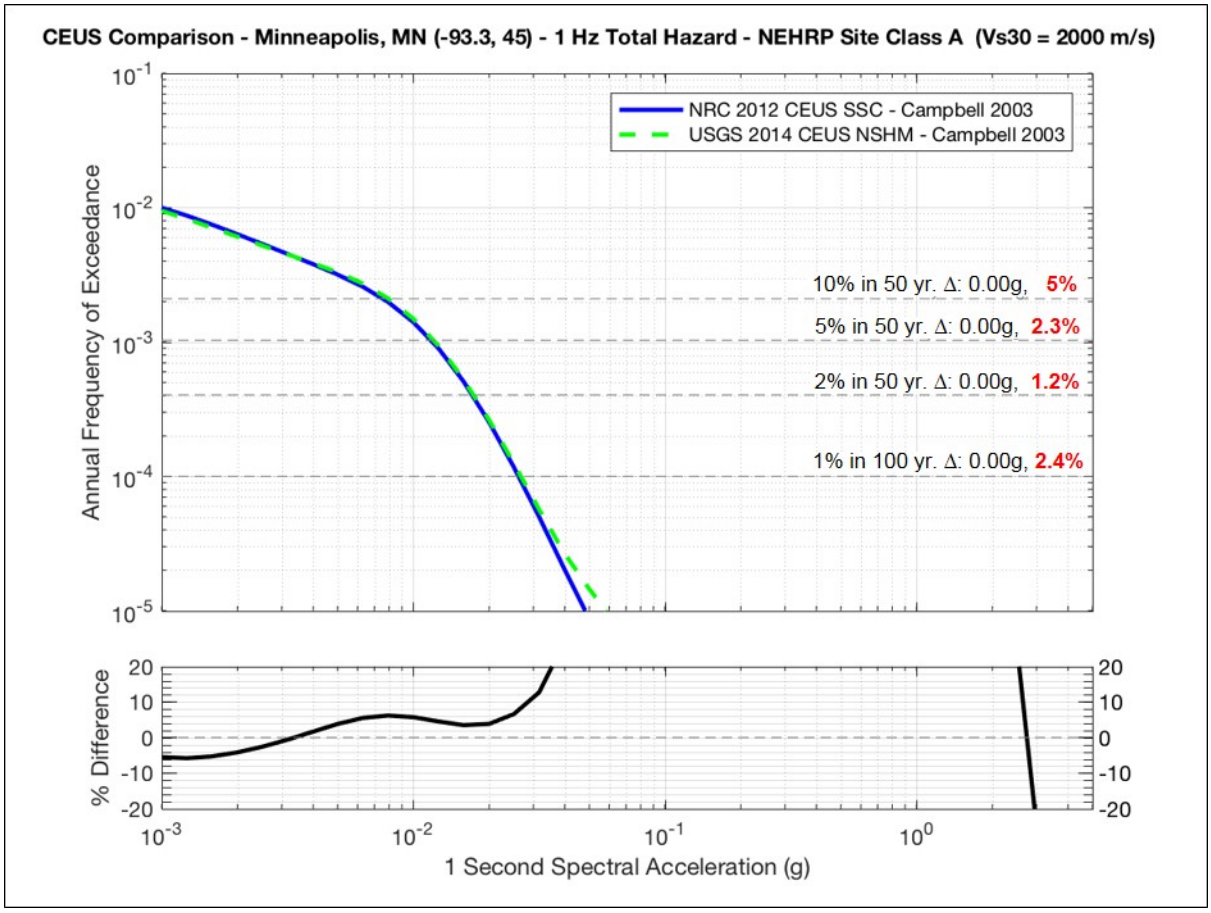

Figure 5-5: Comparison of USGS and NRC 1 Hz hazard curves, considering only the Campbell (2003) ground-motion model, at Minneapolis, MN. The site is located where the USGS and NRC gridded seismicity source model earthquake rates are close to their floor, or minimum, rate. The numbers in red are the ratio of USGS to NRC ground-motion levels at the specified return periods. The lower plot shows the ratio of USGS to NRC exceedance rates over the entire curve (the ratios are mostly out of range of the plot limits).

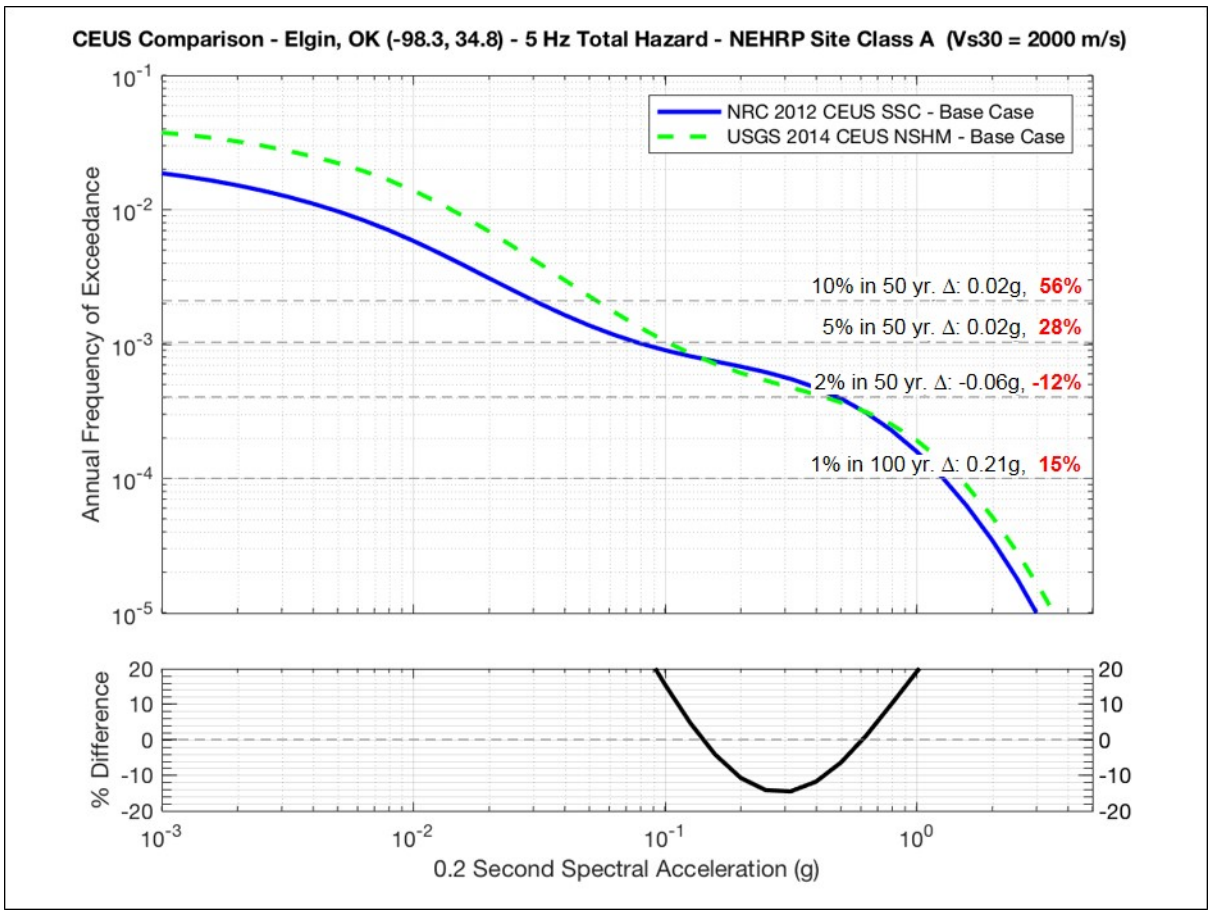

Figure 5-6: Comparison of USGS and NRC 5 Hz hazard curves, considering all ground-motion models, at Elgin, OK. The Elgin site reflects the influence of the Meers fault (USGS) and RLME (NRC). The numbers in red are the ratio of USGS to NRC ground-motion levels at the specified return periods. The lower plot shows the ratio of USGS to NRC exceedance rates over the entire curve (the ratios are out of range of the plot limits).

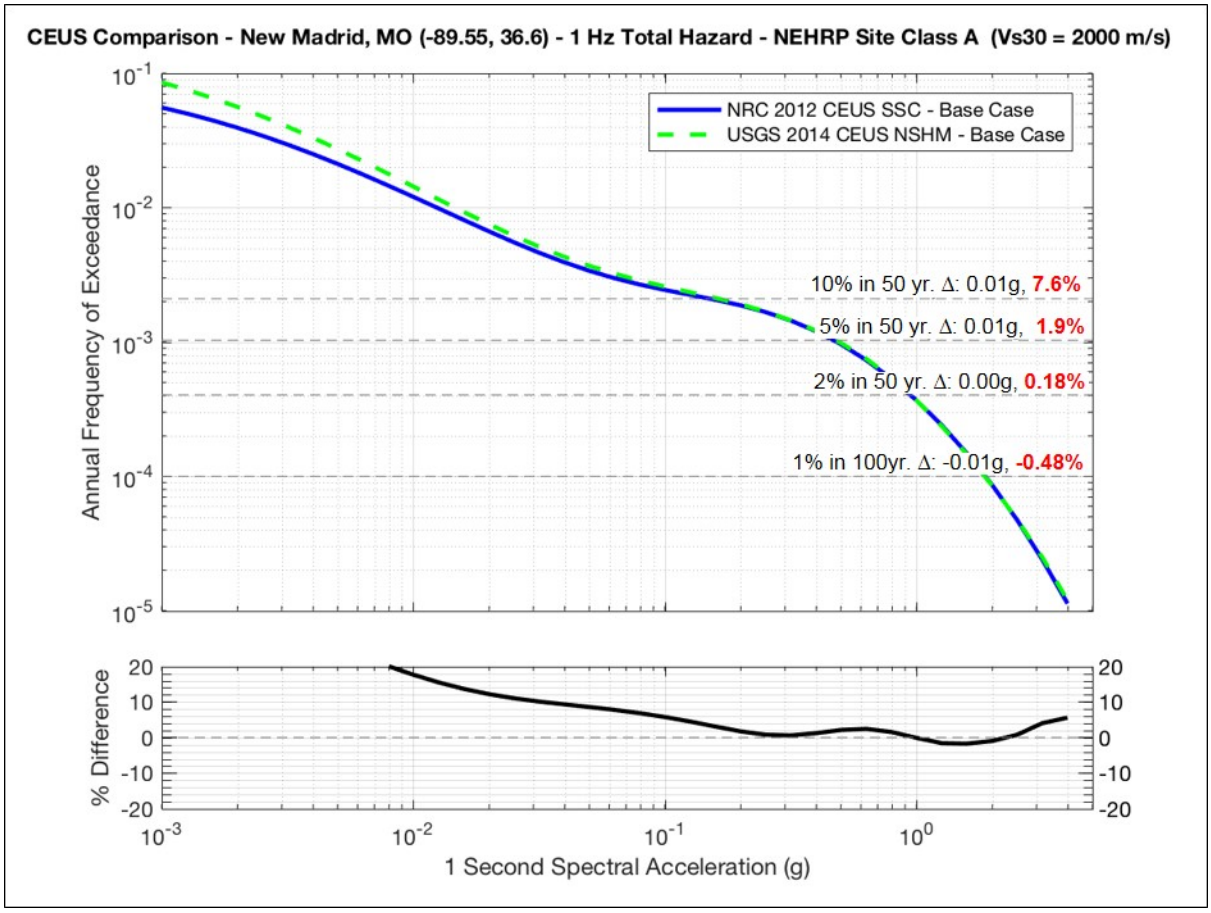

Figure 5-7: Comparison of USGS and NRC 1 Hz hazard curves, considering all ground-motion models, at New Madrid, MO. The New Madrid site is located where the USGS and NRC gridded seismicity source model earthquake rates are close to their floor, or minimum, rate. The numbers in red are the ratio of USGS to NRC ground-motion levels at the specified return periods. The lower plot shows the ratio of USGS to NRC exceedance rates over the entire curve.

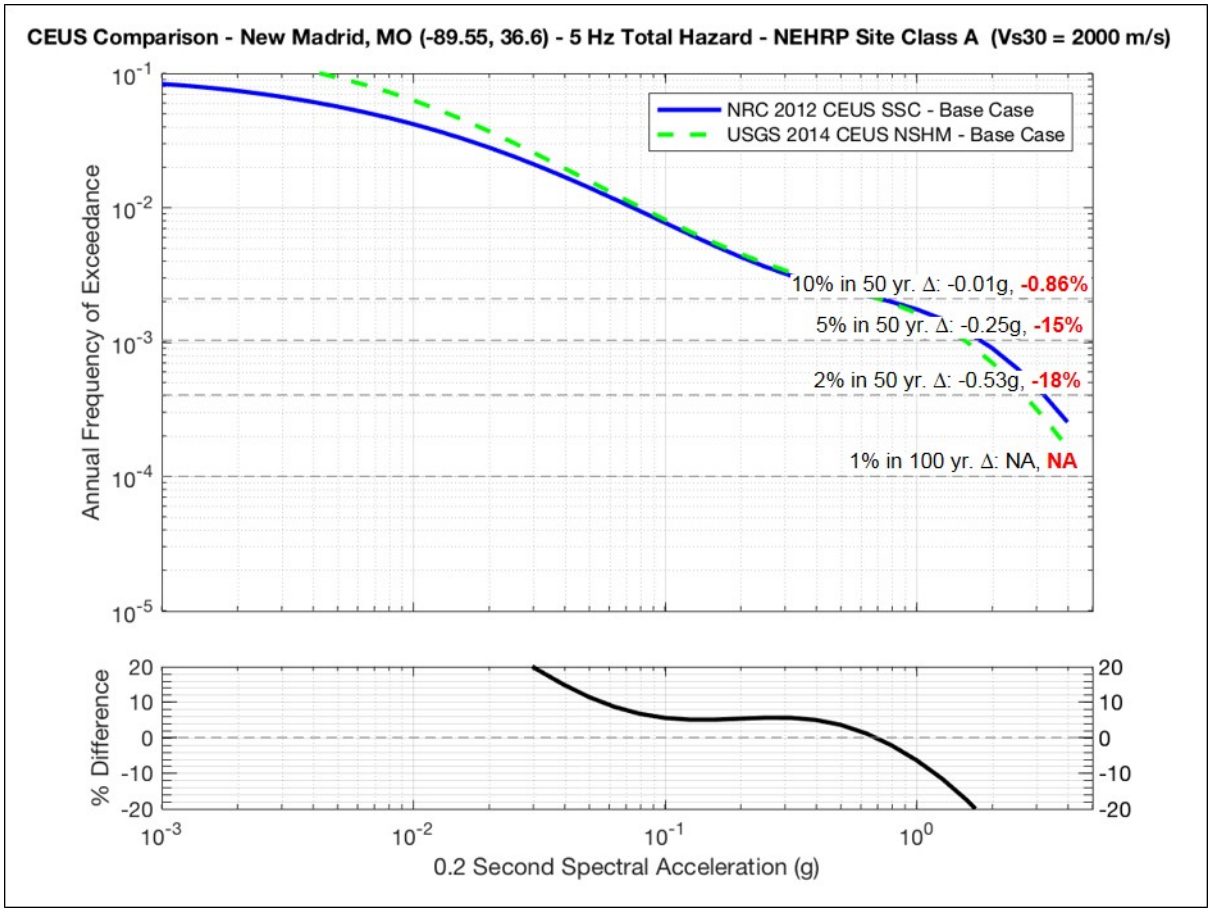

Figure 5-8: Comparison of USGS and NRC 5 Hz hazard curves, considering all ground-motion models, at New Madrid, MO. The New Madrid site is located where the USGS and NRC gridded seismicity source model earthquake rates are close to their floor, or minimum, rate. The numbers in red are the ratio of USGS to NRC ground-motion levels at the specified return periods. The lower plot shows the ratio of USGS to NRC exceedance rates over the entire curve.

6 POTENTIALLY INDUCED EARTHQUAKES (TASK-5A)

6.1 Background

The NRC has the need to investigate the implications of the increase in seismicity resulting from induced earthquakes in the CEUS on seismic hazard estimates and on the methodology used to incorporate induced seismicity and aftershocks into hazard estimates. Therefore, the USGS was tasked with performing research on potentially induced earthquakes in the CEUS through the following activities:

1. Compile recent ground motion records and compare with similar ground motion data or GMMs from natural earthquakes. This residual analysis will help determine the GMMs appropriate for use in estimating hazard from induced earthquakes.
2. Develop alternative hazard models for induced seismicity. This would involve sensitivity studies obtained using: (1) potentially induced earthquakes removed (base case); (2) potentially induced earthquakes included using (a) short-term rates and (b) long term rates; (3) potentially induced earthquakes with decay rate parameter. Additionally, USGS will consider sensitivity studies applying alternative maximum magnitudes and b-values in estimating the activity rates.

6.2 Deliverables

The USGS assembled a database of instrumentally recorded ground motion intensity measurements from induced earthquakes in Oklahoma and Kansas (Moschetti et al., 2016). The database contains uniformly processed ground motion intensity measurements (peak horizontal ground motions and 5-percent-damped PSA for oscillator periods 0.1–10 s). The earthquake event set includes more than 3800 $M \geq 3$ earthquakes in Oklahoma and Kansas from January 2009 to December 2016. Ground-motion time series were collected out to 500 km. USGS also relocated the majority of the earthquake hypocenters using a multiple-event relocation algorithm to produce a set of near-uniformly processed hypocentral locations. The data can be retrieved from the USGS Science Data Catalog: https://www.sciencebase.gov/catalog/item/57f7d8f2e4b0bc0bec09d04d.

Details about data processing are reported in the accompanying article by Rennolet et al. (2018): https://pubs.er.usgs.gov/publication/70195681.

USGS scientists then conducted comparisons of ground motion recordings against an exhaustive set of ground motion prediction equations (GMPEs). Results of these studies are presented in an attached PowerPoint presentation (McNamara, 2018a) and a published abstract (McNamara, 2018b) – a companion scientific publication is in review at BSSA. USGS evaluated, ranked and weighted over 50 CEUS and western US GMMs using two well-established probabilistic methods (log likelihood, LLH), and multivariate LLH (MLLH)). USGS also computed ground motion residuals for peak ground acceleration (PGA) and one-second pseudospectral acceleration (PSA1.0) using GMMs recently implemented in the USGS NSHMP software system (nshmp-haz, available at https://github.com/usgs/nshmp-haz). LLH and MLLH GMM rankings are consistent and indicate that, in general, newer GMMs with lower standard deviations perform better than older GMMs. NGA-west GMMs tend to fit induced CEUS earthquake ground motions better than older CEUS GMMs while NGA-east GMMs tend to fit CEUS tectonic earthquake ground motions better than from induced earthquakes.

The USGS also conducted a series of sensitivity tests as part of its process of developing a 1-year induced seismicity hazard model. The Open File Report summarizing this work can be found at: https://pubs.er.usgs.gov/publication/ofr20151070 . As part of the process of incorporating induced seismicity into the seismic hazard model, USGS evaluated the sensitivity of the seismic hazard from induced seismicity to five parts of the hazard model: (1) the earthquake catalog, (2) earthquake rates, (3) earthquake locations, (4) earthquake $M_{\max}$ (maximum magnitude), and (5) earthquake ground motions. Alternative input models for each of the five parts are described, representing differences in scientific opinions on induced seismicity characteristics. In this report, however, USGS did not weight these input models to come up with a preferred final model. Instead, we present a sensitivity study showing uniform seismic hazard maps obtained by applying the alternative input models for induced seismicity. Weighted models were produced separately and are reported on for 2016, 2017, and 2018 as follows:

2016: https://pubs.er.usgs.gov/publication/70189528

2017: https://pubs.er.usgs.gov/publication/70189533

2018: Petersen et al. (2018).

6.3 References

Petersen, M. D, C. S. Mueller, M. P. Moschetti, S. M. Hoover, K. S. Rukstales, D. E. McNamara, R. A. Williams, A. M. Shumway, P. M. Powers, P. S. Earle, A. L. Llenos, A. J. Michael, J. L. Rubinstein, J. H. Norbeck, and E. S. Cochran (2018). 2018 One-Year Seismic Hazard Forecast for the Central and Eastern United States from Induced and Natural Earthquakes, *Seismo. Res. Lett.*, **89**, 1049-1061. https://doi.org/10.1785/0220180005.

Moschetti, M. P., S. M. Hoover, and C. S. Mueller (2016). Likelihood testing of seismicity-based rate forecasts of induced earthquakes in Oklahoma and Kansas, *Geophys. Res. Lett.*, **43**, 4913–4921, doi: 10.1002/2016GL068948.

Rennolet, S.B., M. P. Moschetti, E.M. Thompson, and W. Yeck (2018). A flatfile of ground motion intensity measurements from induced earthquakes in Oklahoma and Kansas, *Earthquake Spectra,* **34**, doi: 10.1193/101916EQS175DP.

7 THE INFLUENCE OF AFTERSHOCKS ON HAZARD (TASK-5B)

7.1 Background

The influence of foreshocks and aftershocks on hazard is dependent on the productivity of these dependent events. In practice, the method developed by Boyd (2012) is dependent on how the earthquake catalog is declustered. To be consistent with the USGS National Seismic Hazard Maps, Boyd's method uses the Gardner and Knopoff (1974) declustering algorithm, which was derived for California catalogs. Recently, Boyd (2012)found that the Gardner and Knopoff (1974) declustering space and time windows may be too small for central and eastern US earthquake catalogs implying that the proportion of dependent to independent events is greater in the CEUS than found in previous iterations of the USGS maps. The purpose of this task was to study the impact of current and new declustering algorithms on producing a statistically independent set of earthquakes in the CEUS. This could result in a better assessment of aftershock productivity and hazard, regional b-value, the rate of large mainshocks, and uncertainty in earthquake rates.

7.2 Deliverables

The work under this task was not fully funded by the NRC before the end of the period of performance. As a result, work on aftershock declustering was focused principally on the questions tied to one-year hazard forecasts and the differences resulting from use of the full catalog versus a Gardner-Knopoff declustered catalog on hazard estimates. Results of this work are documented in Petersen et al., 2018 referenced below.

7.3 References

Oliver, O.S. (2012). Including Foreshocks and Aftershocks in Time-Independent Probabilistic Seismic-Hazard Analyses, *Bull. Seismo. Soc. Am.*, **102**, 909-917, doi: 10.1785/0120110008.

Gardner, J. K., and L. Knopoff (1974). Is the sequence of earthquakes in southern California, with aftershocks removed, Poissonian? *Bull. Seismo. Soc. Am.*, **64**, 1363–1367.

Petersen, M. D, C. S. Mueller, M. P. Moschetti, S. M. Hoover, K. S. Rukstales, D. E. McNamara, R. A. Williams, A. M. Shumway, P. M. Powers, P. S. Earle, A. L. Llenos, A. J. Michael, J. L. Rubinstein, J. H. Norbeck, and E. S. Cochran (2018). 2018 One-Year Seismic Hazard Forecast for the Central and Eastern United States from Induced and Natural Earthquakes, *Seismo. Res. Lett.*, **89**, no. 3, https://doi.org/10.1785/0220180